We are IntechOpen,
the world's leading publisher of
Open Access books
Built by scientists, for scientists

6,900
Open access books available

186,000
International authors and editors

200M
Downloads

Our authors are among the

154
Countries delivered to

TOP 1%
most cited scientists

12.2%
Contributors from top 500 universities

Interested in publishing with us?
Contact book.department@intechopen.com

Numbers displayed above are based on latest data collected.
For more information visit www.intechopen.com

4

Novel Biomedical Imaging Approach for Detection of Sentinel Nodes in an Orthotopic Xenograft Rat Model of Human Gastric Carcinoma

Akihito Tsubota, Tomoki Koyama, Yoshihisa Namiki,
Norio Tada and Hiroshi Takahashi
Jikei University School of Medicine
Japan

1. Introduction

With advances in endoscopic techniques and the widespread use, detection rates for early gastric carcinoma are increasing, and minimally invasive surgery becomes more important in the treatment. Minimally invasive surgery with less extensive dissection involves avoidance of unnecessary lymphadenectomy, leading to the reduction of postoperative morbidity and mortality rates and the improvement of postoperative quality of life without impairing recurrence-free survival. Sentinel node (SN) biopsy is useful to dissect lymph node (LN) rationally and to avoid unnecessarily extensive lymphadenectomy in surgery for gastric carcinoma, as has been established in breast cancer and melanoma (Krag et al., 1998; Morton, 1992; van der Veen et al., 1994; Veronesi et al., 1997). Thus, SN biopsy could be a promising method for the management of gastric carcinoma. The concept is based on the notion that SNs are the first lymph nodes to which cancer cells metastasize from the primary lesion (Sobin, 2003). The presence of tumor cells in SNs indicates that cancer cells may metastasize to downstream nodes. Conversely, the absence of metastatic tumor cells in SNs indicates that metastasis is unlikely in other nodes. However, a convenient and sensitive method useful for the detection of SNs of gastric carcinoma has not been standardized.

Development of a convenient and sensitive method useful for the detection of SNs will enable surgeons to rationally determine the extent of LN dissection and to perform minimally invasive surgery (Krag et al., 1998; Morton, 1992; van der Veen et al., 1994; Veronesi et al., 1997). Several methods have been developed to detect SNs using radioactive materials or vital dyes, such as patent blue violet, isosulfan blue and indocyanine green in gastric carcinoma (Hayashi et al., 2003; Hiratsuka et al., 2001; Hundley et al., 2002; Ichikura et al., 2002; Isozaki et al., 2004; Karube et al., 2004; Kim, M.C. et al., 2004; Kitagawa & Kitajima, 2002; Lee et al., 2005; Miwa et al., 2003; Nimura et al., 2004; Osaka et al., 2004; Ryu et al., 2003; Simsa et al., 2003; Song et al., 2004; Tanaka et al., 2004). Although the sensitivity of these materials or dyes for the detection of SNs is high, sentinel node navigation surgery using dye- or radio-guided methods has not yet been widely performed in early gastric cancer, partly owing to false-negative results in detecting SNs with tumor cell metastases, or

due to their own inherent drawbacks, such as blurred visualization and/or legal restrictions (Hayashi et al., 2003; Hiratsuka et al., 2001; Ichikura et al., 2002; Kim, M.C. et al., 2004; Kitagawa & Kitajima, 2002; Miwa et al., 2003; Tanaka et al., 2004). Accordingly, standardized tracers remain to be determined.

Photosensitizers are used for the treatment of various carcinomas in a remedy that is well known as photodynamic therapy (Fisher et al., 1995; Kvam et al., 1990; Sharman et al., 1999). Photosensitizing agents preferentially accumulate in tumor tissues, and elicit cytocidal effects on tumor cells when excited at a wavelength specific for each agent (Sharman et al., 1999). Photodynamic therapy makes use of photosensitizers with these unique properties to achieve highly selective and localized treatment of various carcinomas (Sharman et al., 1999). ATX-S10Na (II) is a hydrophilic chlorine derivative with a major absorption wavelength of approximately 670 nm, and emits red fluorescence when excited at its absorption wavelength. ATX-S10Na (II) has been developed as a second-generation photosensitizer, which is eliminated more rapidly from the body than previously known first-generation photosensitizers. Therefore, major adverse reactions such as skin photosensitivity have been markedly reduced, compared to those of the first generation photosensitizers (Matsumoto et al., 2003; Mori et al., 2000a, 2000b; Nakajima et al., 1992, 1998). In addition, ATX-S10Na (II) has a high affinity and specificity for tumor tissues, and thereby selectively accumulates in tumor tissues (Matsumoto et al., 2003; Mori et al., 2000a, 2000b; Nakajima et al., 1992, 1998). To our knowledge, our study was the first report that describes the use of a hydrophilic photosensitizer, ATX-S10Na (II), for the detection of SNs in orthotopic transplants of human gastric carcinoma (Koyama et al., 2007a).

In the present chapter, we showed a novel fluorescence-guided imaging system to detect SNs using a photosensitizing agent, ATX-S10Na (II), as a novel fluorescent tracer, and its usefulness for a fluorescence-guided lymphatic mapping system in an animal model of human gastric carcinoma. In the model, human gastric carcinoma cells were implanted orthotopically into nude rats. ATX-S10Na (II) was injected subserosally into the primary tumor lesion, and visualized by a fluorescence spectrolaparoscope. ATX-S10Na (II) would serve as a novel tracer in sentinel node navigation surgery for gastric carcinoma.

1.1 Concept of sentinel node

The sentinel node (SN) is defined as the first lymph node (LN) to receive lymphatic drainage from a primary tumor, and therefore it is commonly accepted that SN is the first LN in which tumor cells from the primary lesion form lymphatic metastases (Sobin, 2003; Fig. 1). Detection of a metastatic tumor in the SN could mean metastasis of tumor cells to the downstream LNs. Conversely, absence of metastatic tumors in the SN indicates that the downstream LNs most likely do not contain metastatic tumor cells.

2. Photosensitive fluorescent tracer

ATX-S10Na (II) [13,17-bis(1-carboxypropionyl) carbamoylethyl-8-ethenyl-2-hydroxy-3-hydroxy-iminoethylidene-2,7,12,18-tetramethyl-prophyrin tetrasodium salt], is synthesized, purified and supplied by Photochemical Co. (Okayama, Japan). Its structure ($C_{42}H_{41}N_7Na_4 O_{12}$; molecular weight 927.77, Fig.2) and metabolism were described in detail previously (Matsumoto et al., 2003; Mori et al., 2000a, 2000b; Nakajima et al., 1992, 1998). When the photosensitizer is activated by irradiation with excitation light of 450±40 nm (mean ± SD), it emits a strong red fluorescence of 667 nm wavelength (Fig. 3). Therefore, we are able to

Novel Biomedical Imaging Approach for Detection
of Sentinel Nodes in an Orthotopic Xenograft Rat Model of Human Gastric Carcinoma
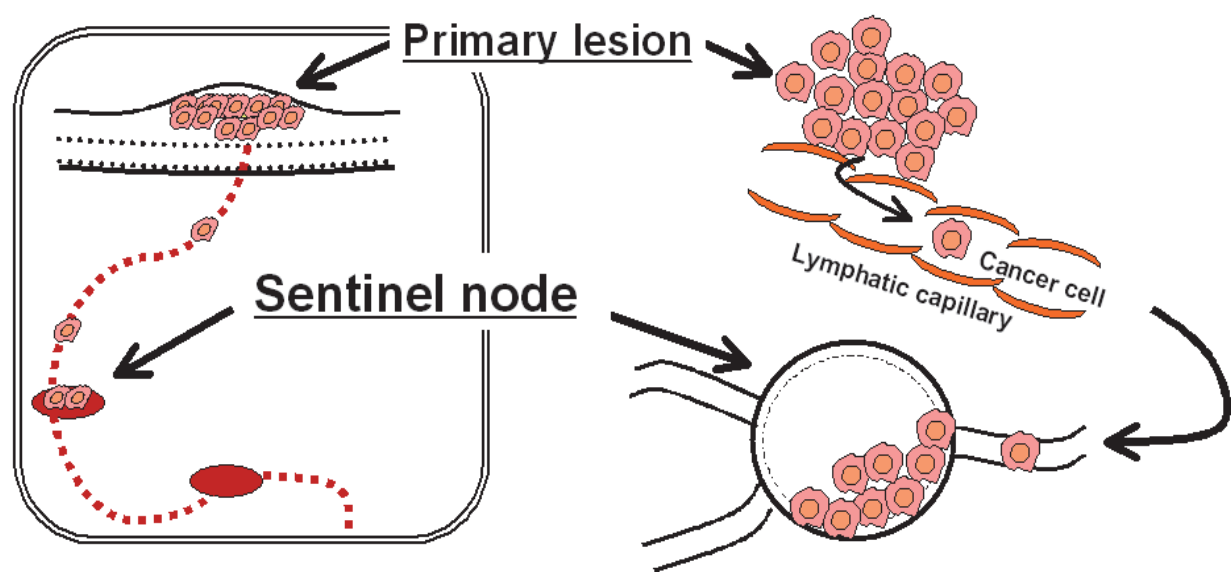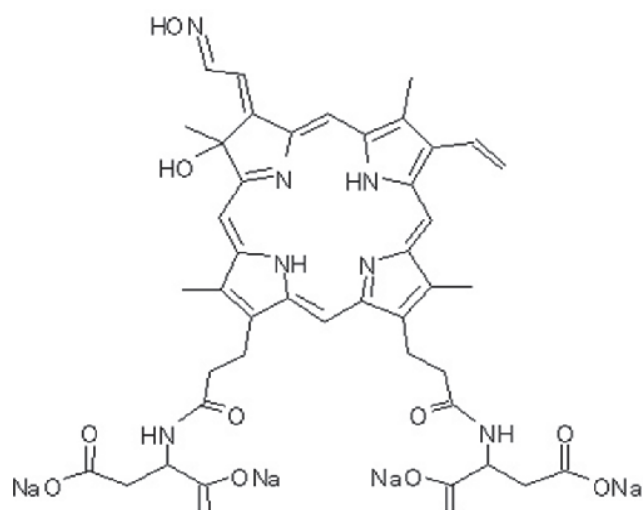
57

Fig. 1. Concept of sentinel node

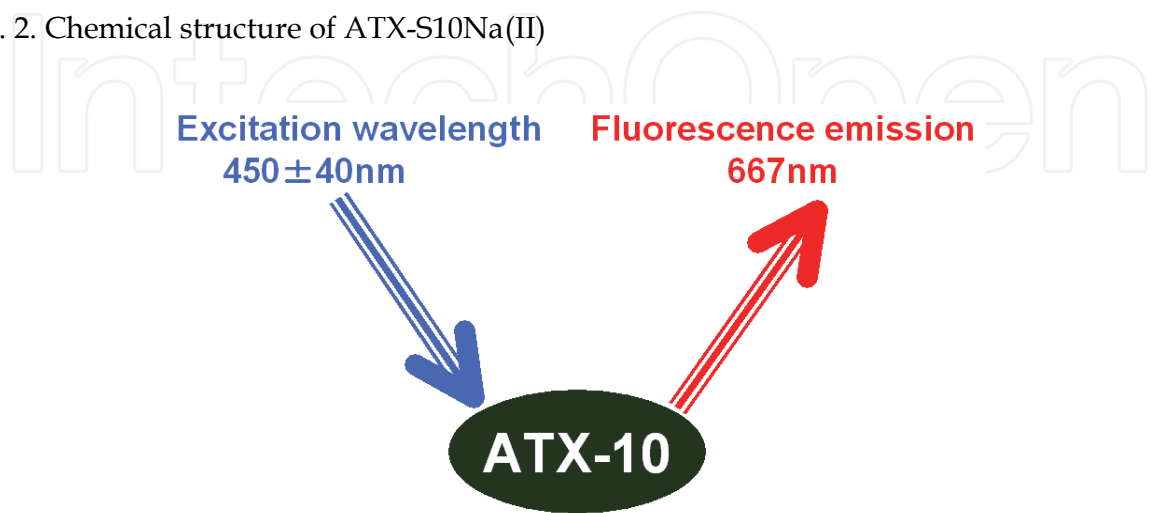Fig. 2. Chemical structure of ATX-S10Na(II)

Fig. 3. Basic principle of photosensitizer

detect the sentinel node by the red fluorescence of ATX-S10Na (II) which is injected at the primary tumor. The reagent is stored as a powder in the dark at -80°C, and dissolved in phosphate-buffered saline to a final concentration of 5 mg/ml each time immediately before use.

3. Orthotopic xenograft model of human gastric carcinoma

3.1 Cell line

The OCUM-2M LN cell line was originally derived from human scirrhous gastric carcinoma (Fujihara et al., 1998). This cell line forms LN metastases, when it is injected orthotopically into the stomach of athymic nude rats. Cells are cultured in Dulbecco's modified Eagle's medium (DMEM) supplemented with 10% fetal calf serum, 100 U/ml penicillin, and 100 mg/ml streptomycin in a humidified atmosphere containing 5% CO_2 at 37°C. The cells in the log phase of growth are washed twice with phosphate-buffered saline, treated with trypsin and collected by centrifugation. The cell pellets are dissolved in DMEM and adjusted at a concentration of 5×10^7 cells/ml. Cells are used in the experiments only when their viability exceeds 95%, as determined by the trypan blue dye-exclusion test.

3.2 Tumor cell implantation

Five- to seven-week-old female athymic nude rats (F344/N Jcl-*rnu*; CLEA Japan, Co., Tokyo, Japan) are housed in a temperature-controlled pathogen-free facility, maintained on a 12-hour light/12-hour dark cycle, and provided with commercially available rat chow and tap water *ad libitum*. Rats are pretreated by irradiation with 3 Gy of X-rays 3 days before tumor cell inoculation to reduce the number of active natural killer lymphocytes (Fig. 4). Rats are anesthetized for all procedures by an intraperitoneal injection of pentobarbital sodium (40 mg/kg body weight), and then an incision is made in the upper abdominal median line. The stomach is exposed, and a total of 1×10^6 OCUM-2M LN cells in a volume of 20 µl of DMEM is injected subserosally into the middle anterior wall of the lesser curvature of the stomach with a 29-gauge needle. After the orthotopic implantation of tumor cells, the abdominal wall is sutured and closed using 6-0 surgical sutures. All procedures are performed in a pathogen-free environment. To monitor the growth of inoculated tumor cells, sera are obtained by periorbital bleeding weekly, and the serum levels of CA19-9, a marker of tumor growth, are
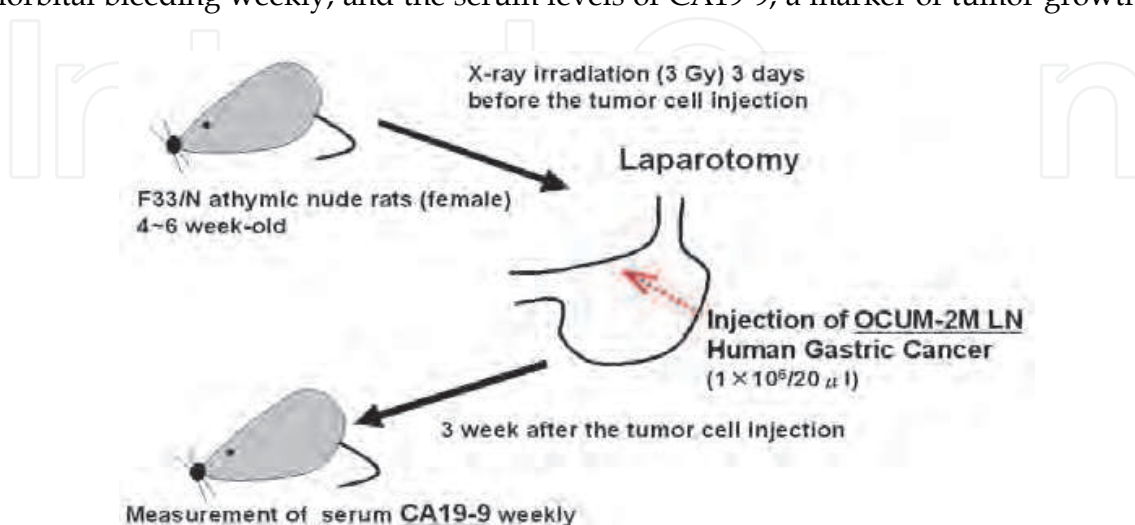

Fig. 4. Procedures of tumor cell implantation

Novel Biomedical Imaging Approach for Detection
of Sentinel Nodes in an Orthotopic Xenograft Rat Model of Human Gastric Carcinoma

59

measured by radioimmunoassay using a commercially available kit (Fujirebio, Inc., Tokyo). When the level of serum CA19-9 values increases above 6 units/ml, which is a sign of tumor growth, the presence of SNs is investigated with a fluorescence spectrolaparoscope.

3.3 Establishment of orthotopic xenograft

In our experiment, 95% of nude rats inoculated with tumor cells showed the establishment of orthotopic xenografts of human gastric carcinoma (Koyama et al, 2007a). The primary lesions of the implanted tumors grew up to the median size of 5.0 mm (range, 2.2–8.2 mm) by the largest diameter. In tumor-bearing rats, the median size of the left gastric LNs (Lg-LNs) was 3.9 mm (range, 2.5-14.3 mm) in diameter. Fig. 5 shows a representative example of the primary lesion in the stomach and the enlarged Lg-LN. Subserosally inoculated OCUM-2M LN cells developed into a solid tumor ("primary lesion"; Fig. 5, black arrowhead) at the middle anterior wall of the lesser curvature of the stomach. Enlarged Lg-LN (Fig. 5, white arrowhead), which had tumor metastases, was also observed. The corresponding Lg-LN specimen displays poorly differentiated adenocarcinoma, which is a characteristic feature of OCUM-2M LN, human scirrhous carcinoma of the stomach (Fig. 6; bar = 100 µm).

To confirm the presence of tumor cells in LNs (LN metastasis), human β-actin was amplified specifically by cDNA synthesis of total RNA extracted from tissue samples and subsequent reverse transcriptase-polymerase chain reaction (RT-PCR). The LN metastases were histopathologically observed in 56% of tumor-bearing rats. These tissues were positive for human β-actin by RT-PCR (Koyama et al, 2007a). Control rats did not develop solid tumors and showed no changes in the lymphatic system.
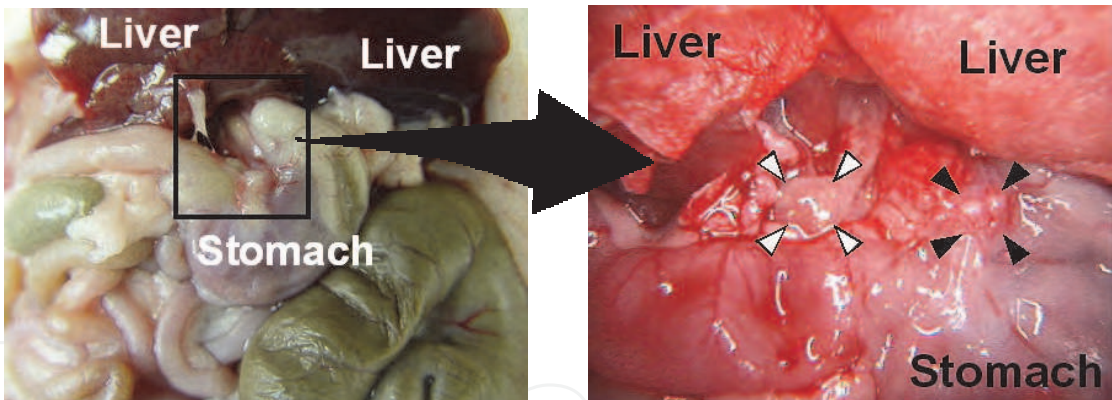

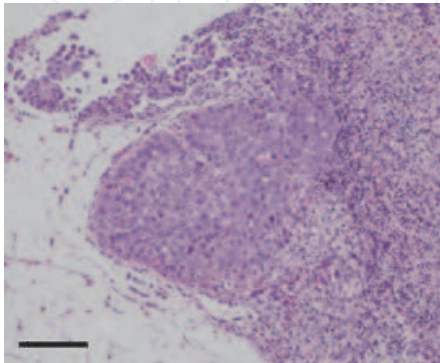Fig. 5. Establishment of orthotopic xenograft model of human gastric carcinoma

Fig. 6. Hematoxylin and eosin stain of left gastric lymph node

4. Detection of sentinel nodes by fluorescence spectrolaparoscope

4.1 Fluorescence spectrolaparoscope

Re-laparotomy is performed on tumor-implanted rats under general anesthesia, when serum CA19-9 concentrations increase above 6 units/ml. After an exposure of the stomach, ATX-S10Na(II) solution at a total volume of 40–60 µl is injected using a 29-gauge needle into the serosal side of the implanted tumor [Fig. 7(a)]. ATXS10Na(II) injected into the primary lesion is excited by the light of 450±40 nm [Fig. 7(b), 7(c) and 7(d)], which is emitted from the tip of the laparoscope equipped with a xenon lamp and a bandpass excitation filter of 450±40 nm. ATX-S10Na(II) localized in tissues emits fluorescence of 667 nm, which is visualized using a bandpass emission filter of >510-nm. The emission filter is useful for blocking the excitation light and other components such as natural autofluorescence of the surrounding tissues. An image-intensified charge-coupled device (CCD) camera is furnished with two built-in filters, a conventional white-light filter and an emission filter of >510-nm, and is attached to the ocular end of the laparoscope through the adaptor. The dynamic image of excited ATX-S10Na(II) is monitored in real-time on an RGB display via an image processing system, and recorded on a camcorder with 192×10^4 pixels for 60 minutes after the injection. The intensity and exposure time of the excitation light are constant throughout these experiments.

4.2 Dynamic imaging and distribution of photosensitizer

Fluorescence distribution of ATX-S10Na(II) in the abdomen is visualized as vivid red color on the imaging board using the spectrolaparoscope. In tumor-bearing rats, ATX-S10Na(II) solution is injected into the tumor of primary lesion via stomach serosa using a 29-gauge syringe [Fig. 7 (a); white arrowhead]. The red-fluorescent ATX-S10Na(II) is clearly identified and uptaken rapidly into the lymphatic tissue around the primary lesion [Fig. 7 (b)]. Subsequently, the red-emitting fluorescence is incorporated rapidly into the Lg-LN [Fig. 7 (c) and (d); white arrowhead] through the afferent lymphatic vessels [Fig. 7 (c) and (d); white arrows]. The migration of ATX-S10Na(II) takes place within a period of 5 minutes of the injection. The fluorescence intensity increases, reaching a peak and plateau approximately at 1–9 minutes, and persists without attenuation during the entire observation time. In contrast, no or little fluorescence is detected in the surrounding non-lymphatic tissues. The contrast between the red fluorescent tissues and non-fluorescent area is distinct, and all investigators can identify the red fluorescent nodes easily. In control rats, fluorescent dye is incorporated rapidly into the lymph vessels around the injection site, migrates through them and disappears within 3 minutes. Of note, none of the LN is stained with the fluorescence in the control rats.

4.3 Sentinel nodes and nodal metastases

According to the sentinel node (SN) concept, the first LN into which ATX-S10Na(II) flows is regarded as the "SN". Fig. 8 shows an example in which ATX-S10Na(II) was incorporated rapidly into afferent lymphatic vessels around the primary lesion, lymphatic network, and flowed first into the Lg-LN. Thus, the Lg-LN was regarded as the SN. The Lg-LN was occupied with tumor cell metastases, showing poorly differentiated adenocarcinoma with a characteristic feature of OCUM-2M LN, human scirrhous carcinoma of the stomach [Fig. 8 (d); hematoxylin and eosin stain], and was visualized by the red-fluorescence of ATX-S10Na (II) [Fig. 8 (a), (b) and (c)]. The incision was made in the isolated red-fluorescent Lg-LN at

(a) Injection of ATX-S10Na(II)   (b) Uptake into lymphatic tissue

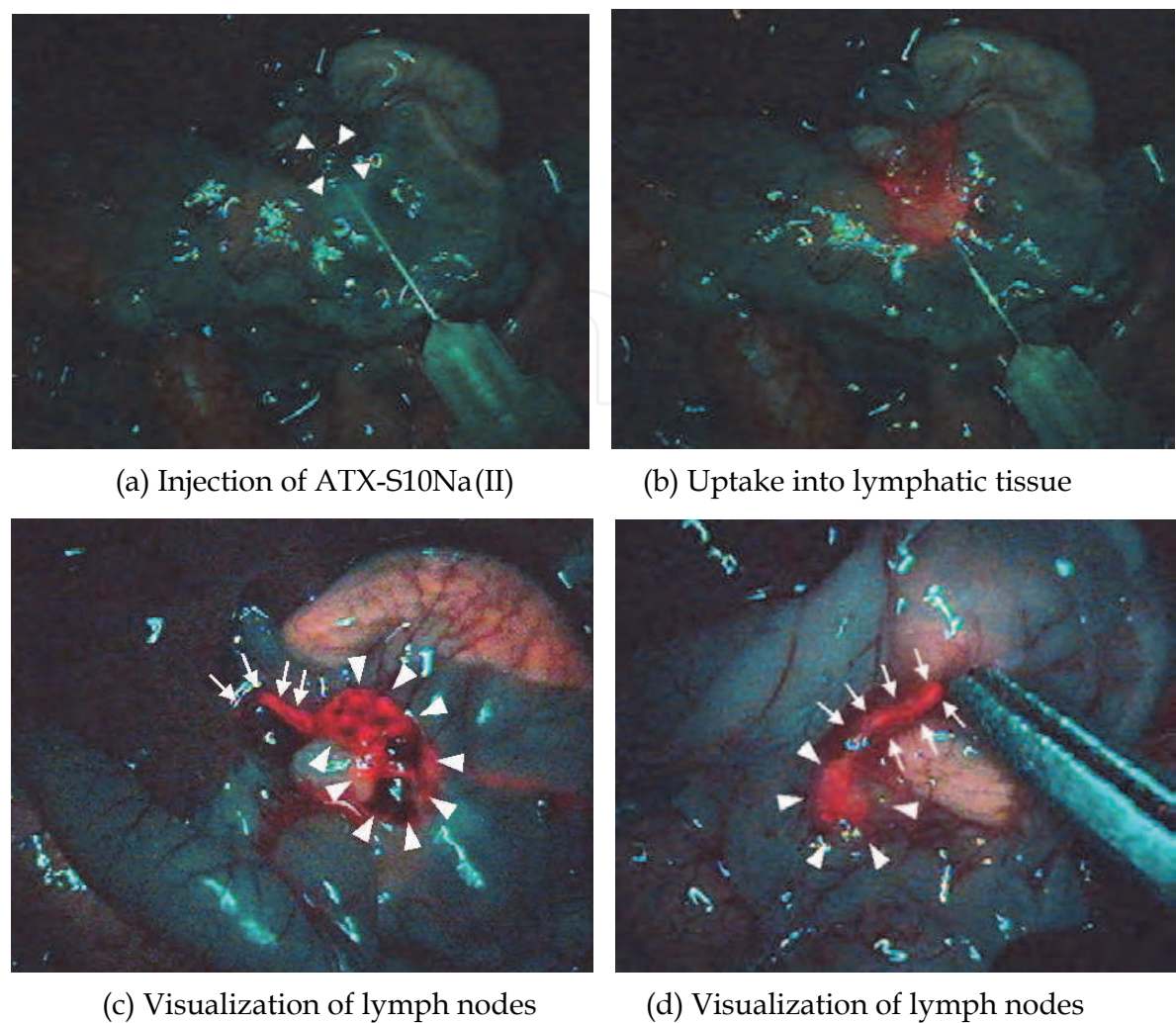(c) Visualization of lymph nodes   (d) Visualization of lymph nodes

Fig. 7. Detection of lymphatic tissues by ATX-S10Na(II)

the dotted line [Fig. 8 (b)], and the uptake of red fluorescence into metastatic lesion was observed as shown in Fig. 8 (c) and (d). We provisionally termed the red-fluorescent LNs "red nodes", similar to those designated as "blue or green nodes" using vital dyes (Hayashi et al., 2003; Hiratsuka et al., 2001; Ichikura et al., 2002) or "hot nodes" using radioactive particles (Hayashi et al., 2003).

After the completion of each experiment, the Lg-LN (SN) was separated, and the other LNs located downstream of Lg-LN or SN, including the hepatic, splenic and pancreatico-duodenal LNs, were harvested *en bloc*. In all LN samples dissected, the presence of human β-actin mRNA was investigated by RT-PCR to assess the presence of metastases of tumor cells (Koyama et al., 2007a). In 25 out of 27 rats, ATX-S10Na (II) was incorporated into the Lg-LN (SN), which was identified as a red node. Of note, human β-actin was positive in 24 out of these 25 red nodes (SNs). To our surprise, human β-actin was also positive in all LNs located downstream of human-β-actin-positive red-fluorescent Lg-LNs (SNs) in these 24 rats. In contrast, human β-actin was negative in the downstream LNs of the rat with a human-β-actin-negative red-fluorescent Lg-LN (SN). In the remaining 2 out of 27 rats, the ATX-S10Na (II) was incorporated into the hepatic LNs (SNs), but not into the Lg-LN (non-SN). Therefore, the hepatic LN but not the Lg-LN was identified as a red node (SN) in these two rats. Interestingly, both of the two non-red Lg-LNs (non-SNs) were negative for human
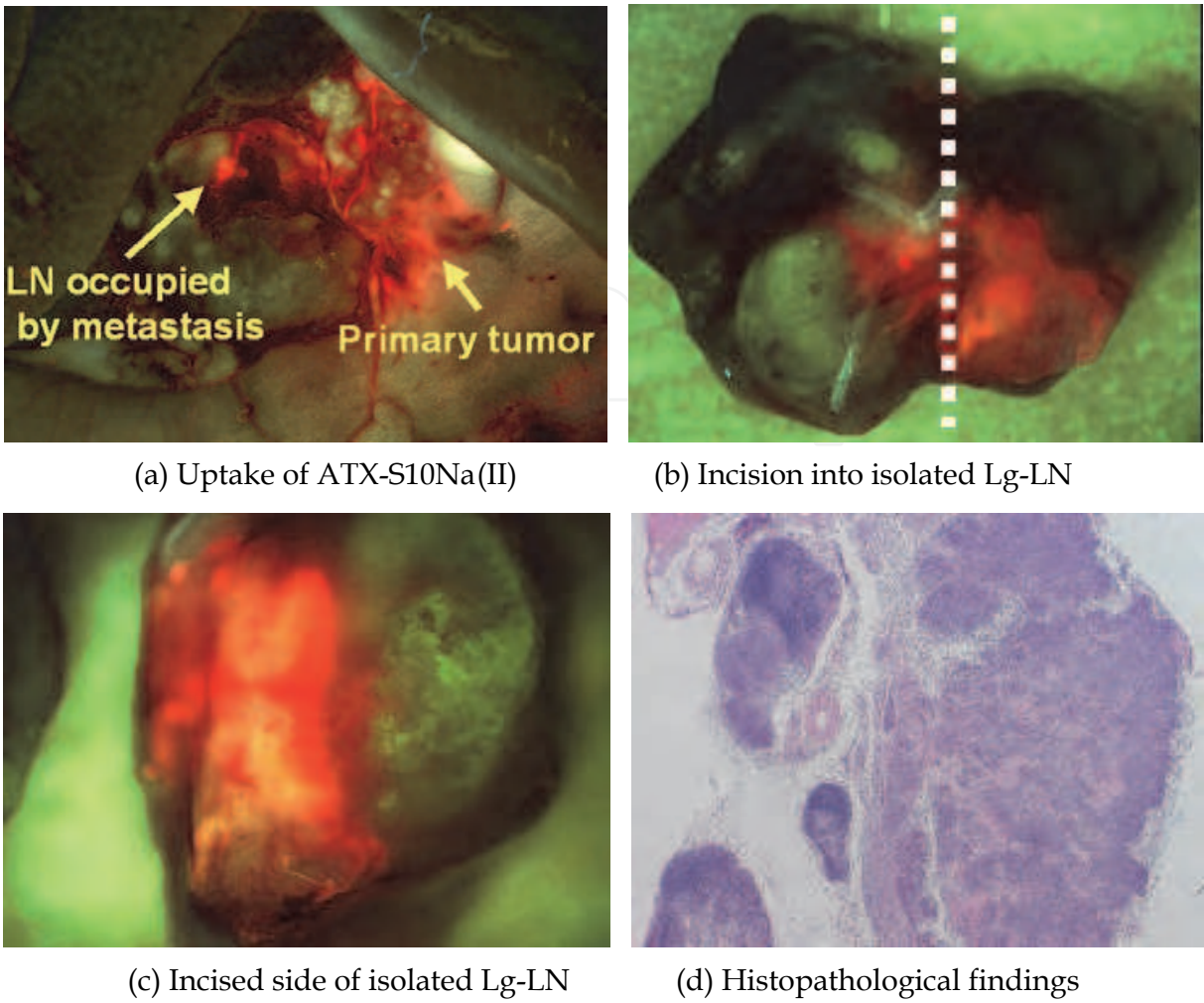
(a) Uptake of ATX-S10Na(II)

(b) Incision into isolated Lg-LN

(c) Incised side of isolated Lg-LN

(d) Histopathological findings

Fig. 8. Lymph nodes detected by ATX-S10Na(II)

β-actin, whereas both of the two red-fluorescent hepatic LNs (SNs) were positive for human b-actin. On the single-section specimens, 19 human-β-actin-positive red-fluorescent Lg-LNs were poorly differentiated adenocarcinoma, and others showed no malignant findings. In control rats, human β-actin was negative in both Lg-LNs and other LNs.
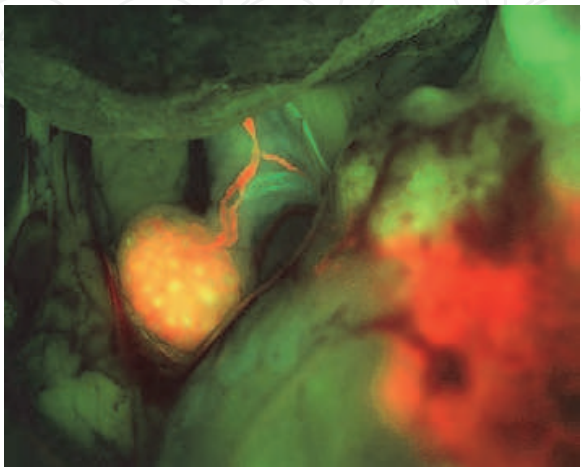

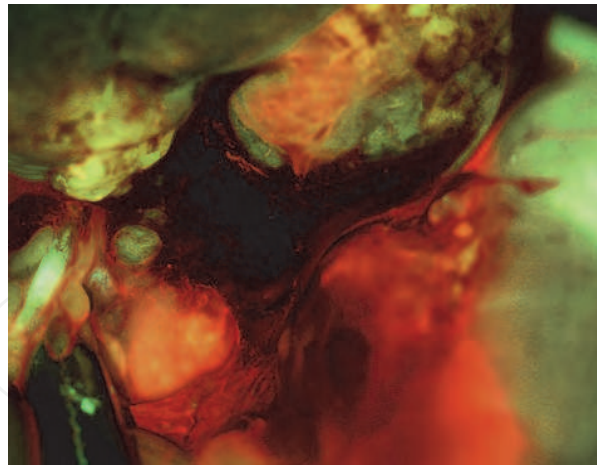Fig. 9. Uptake of ATX-S10Na(II) in Case 1
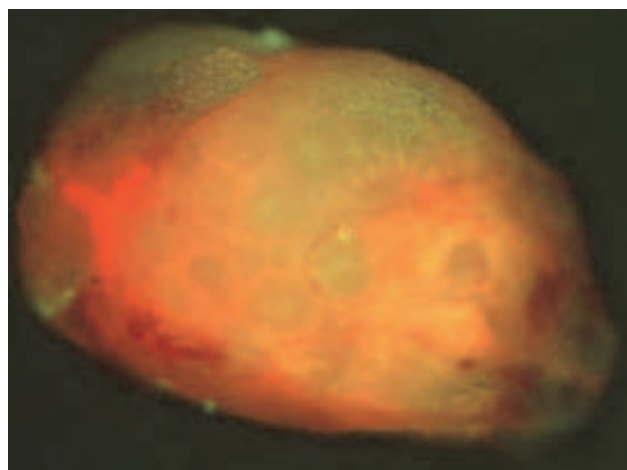
Fig. 10. Uptake of ATX-S10Na(II) in Case 2

Fig. 11. Isolation of red-emitting Lg-LN stained with ATX-S10Na(II)

In another two examples (Fig. 9 and 10), red-fluorescent ATX-S10Na (II) was incorporated rapidly into afferent lymphatic vessels around the primary lesion, lymphatic network, and flowed first into the Lg-LN. The lymph nodes as well as afferent lymphatic vessels were visualized vividly by this method. Although Case 2 (Fig. 10) was bleeding heavily during experiment, red-emitting LNs were detected easily. After the completion of observation, a red-emitting Lg-LN with metastasis of poorly differentiated adenocarcinoma was harvested and dissected in Case 1 (Fig. 11). The LN continued to emit red fluorescence in the similar degree of intensity at least for 30 minutes. Thus, ATX-S10Na (II) could efficiently visualize lymphatic network around the primary lesion, afferent lymphatic vessel and sentinel node. This method is simple and convenient, since it dose not require radioisotope or gamma probe.

5. Advantage of photosensitizer to tracer

5.1 Visualization of sentinel nodes by strong emission of red fluorescence

ATX-S10Na (II) emits strong red fluorescence with excitation wavelength (Nakajima et al., 1998). As shown in Fig. 7 to 10, the distribution of ATX-S10Na (II) in lymphatic network can be detected clearly and easily by the red fluorescence marking. This photographic visualization allows any observer to clearly identify SNs, and to easily determine the

location and orientation of SNs in the orthotopic xenograft animal model. Such direct real-time visualization is not possible using radioactive tracers, which must be measured by scintillation probes or gamma camera (Hayashi et al., 2003; Kim et al., 2004; Kitagawa & Kitajima, 2002; Tanaka et al., 2004). Of note, this novel procedure would be easily conducted in human and in community hospitals without difficulties, because it does not require complicated procedures, special facilities or radioactive substances. Other non-fluorescent dye tracers (Hiratsuka et al., 2001; Ichikura et al., 2002; Hayashi et al., 2003; Miwa et al., 2003; Tanaka et al., 2004) cannot provide such a vivid and colorful contrast. The visual and technical advantage of ATX-S10Na (II) may assist every surgeon to assess SNs accurately in sentinel node navigation surgery, and potentially prevent an oversight for false-negative LNs.

5.2 Rapid incorporation into lymphatic tissues

As a general rule, photosensitizers are systemically administered via a peripheral intrave-nous route before laser irradiation in photodynamic therapy for various carcinomas. As shown in Fig. 7, however, ATX-S10Na(II) is incorporated rapidly into lymphatic tissues after subserosal injection into the primary tumor. Our study confirmed for the first time that ATX-S10Na (II) is taken up by local lymphatic tissues when it is subserosally injected into the primary tumor lesion (Koyama et al., 2007a). One possible explanation for the phenomenon is that the chemical structure of ATX-S10Na(II) is water-soluble, but not lipid-soluble (Matsumoto et al., 2003; Mori et al., 2000a, 2000b; Nakajima et al., 1992, 1998). Since the uptake of ATX-S10Na (II) into lymphatic system is rapid and its fluorescence can be consistently observed in real time, this approach appears to be useful for shortening the time required for SN biopsy and surgical procedure. Of importance, the ATX-S10Na (II)-guided method is not associated with the "shine-through" phenomenon, whereby the large hot spot at the injection site of radioactive tracers disturbs the detection of SNs around the primary tumor lesion.

5.3 High affinity and specific uptake to tumor cells

ATX-S10Na (II) is a high affinity molecule for tumor cells. Its preferential uptake in target tumor cells results in selective accumulations in tumor tissues, indicating that the tumor-specificity of photodynamic therapy depends largely on the oncotropic properties of photo-sensitizers (Fisher et al., 1995; Kvam et al., 1990; Matsumoto et al., 2003; Mori et al., 2000a, 2000b; Nakajima et al., 1992, 1998; Sharman et al., 1999). As shown in Fig. 8, ATX-S10Na (II) can be taken up by LNs that are involved with tumor metastases. However, the precise mechanisms of tumor-specific uptake of ATX-S10Na (II) remain unclear. It is proposed that ATX-S10 Na (II) is incorporated into tumor cells by fluid phase endocytosis, receptor-mediated endocytosis, or orphan transporters (Mori et al., 2000b). Alternatively, another possible mechanism is that lymphatic flow is delayed or altered in LNs filled with metastatic tumor cells, resulting in preferential retention of ATX-S10Na (II) in such LNs. In our previous study, the presence of tumor metastases in LNs was assessed by RT-PCR of human β-actin (Koyama et al., 2007a). To our surprise, human β-actin was positive in all LNs located downstream of human-β-actin-positive Lg-LN that was regarded as SN. In contrast, LNs located downstream of human-β-actin-negative Lg-LN (SN) were negative for human β-actin. In addition, all human-β-actin-positive Lg-LNs (SNs) were red nodes, whereas all non-red Lg-LNs (non-SNs) were human β-actin-negative. Considering the higher positive

rates by RT-PCR assay than conventional histopathological examination (Bilchik et al., 2001; Kitagawa & Kitajima, 2002; Maruyama et al., 1999; Natsugoe, et al., 1998; Noura et al., 2002), these results showed high sensitivity and specificity of the ATX-S10Na (II)-guided method for the detection of SNs. Because micrometastasis occurs frequently in gastric carcinoma, the system using ATXS10Na(II) may be a novel technology to detect micrometastases with high sensitivity, resulting in reduction of false-negative LNs.

5.4 Little toxicity in human

No obvious toxicity was observed in rats that were injected locally with ATX-S10Na(II) at a dose of 1.3–2.5 mg/kg in our study (Koyama et al., 2007a). This dosage is much smaller than that of systemic administration given intravenously at a dose of 5–25 mg/kg, which caused little, if any, toxicity *in vivo* (Matsumoto et al., 2003; Mori et al., 2000a; Nakajima et al., 1992, 1998). Since ATX-S10Na(II) is a hydrophilic photosensitizer with a low-molecular weight, its clearance from tissues and body (within 24 hours) is much faster than that of the first generation photosensitizers. Therefore, it has substantially less adverse effects (Matsumoto et al., 2003; Mori et al., 2000a; Nakajima et al., 1992; Nakajima et al., 1998). We acknowledge that our studies were conducted in an orthotopic xenograft rat model (Koyama et al, 2007a, 2007b), in which the structure and anatomy of the regional lymphatic network may be different from those of human system (Ichikura et al., 2002; Miwa et al., 2003). Alternatively, the rat model may not be comparable to early gastric carcinoma in humans, for which sentinel node navigation surgery is more suitable (Hiratsuka et al., 2001; Isozaki et al., 2004). Clear visualization of lymphatic system by ATX-S10Na (II) may be only true of the animal model. However, our studies do demonstrate the potential usefulness of ATX-S10Na(II) as a tracer of SNs by assessing tumor metastases with RT-PCR (Koyama et al., 2007a, 2007b). In 25 out of 27 rats, Lg-LN (SN) was identified as a red node, and most of these Lg-LNs (SNs) were positive for human β-actin, which was an indication of tumor metastasis. Of interest, ATX-S10Na(II) was incorporated into the hepatic LN (SN), but not into the Lg-LN (non-SN) in two out of 27 rats, and human β-actin was positive only in the hepatic LN (SN), but not in the Lg-LN (non-SN) in these rats. These findings support the notion that SN is the first LN to receive lymphatic drainage and tumor cells from a primary tumor, and ATX-S10Na (II) is useful for the detection of SNs.

6. Other dye tracers and comparison with ATX-S10Na(II)

Patent blue violet (Hayashi et al., 2003; Karube et al., 2004; Miwa et al., 2003; Simsa et al., 2003), isosulfan blue (Hundley et al., 2002; Isozaki et al., 2004; Lee et al., 2005; Osaka et al., 2004; Ryu et al., 2003; Song t al., 2004) and indocyanine green (ICG) (Hiratsuka et al., 2001; Ichikura et al., 2002; Nimura et al., 2004) have been used as vital dye tracers for the detection of SNs in gastric carcinoma. The detection rates of SNs were 72–96%, 91–100% and 99–100%, respectively. These favorable results must be carefully interpreted because SN mapping is dependent on the technical learning curve and skills of the surgeon (Ichikura et al., 2002; Simsa et al., 2003; Nimura et al., 2004). The sensitivity was 77–90%, 46–100% and 64–90%, respectively, suggesting that non-SNs could contain tumor cell metastases. In most of these reports, the presence of metastasis in LNs was determined by conventional haematoxylin and eosin staining. False-negative rates may increase when more sensitive methods such as multiple sectioning, immunohistochemical staining or RT–PCR technique are used.

Some biomedical imaging techniques use the characteristic feature of ICG; this dye absorbs infrared rays, which enhances its visibility (Flower & Hochheimer, 1976; Kohso et al., 1990). Enhanced visualization of ICG by using a near-infrared endoscopy substantially improves the rate of SN detection in patients with gastric carcinoma, compared with the use of ICG alone (Nimura et al., 2004). Interestingly, SNs illuminated with a near-infrared endoscope are clear enough to be identified by all observers, whereas SNs stained by ICG alone are not always visible to all investigators. As a result, the ICG-guided method combined with a near- infrared endoscope was reported to increase the sensitivity significantly from 64% of patients and 50% of LNs to 100% and 100%, respectively (Nimura et al., 2004). The combination method appears to be a promising approach for biomedical imaging in living tissue.

As shown in Fig. 7 to 10, the rapid migration of ATX-S10Na (II) along the lymphatic system is clearly visualized and easily identified in real time by the strong red fluorescence. Such visualization is clearer than that of enhanced visualization of ICG with a near-infrared laparoscope (Koyama et al., 2007b). Since a much darker operating room is required to ensure the detection of ICG through a near-infrared endoscopy, it may be difficult to perform other procedures. One explanation for the high-quality visualization of ATX-S10Na (II) is that the excitation wavelength peak (450 ± 40 nm) is completely separate from the emission wavelength peak (667 nm). With the visual advantage of ATX-S10Na (II), SNs would not be missed, and the time required for the surgical procedure may be shortened.

In a comparative study using an orthotopic xenograft rat model, there was no significant difference in the detection rates of SNs, the sensitivity, and the number of stained nodes between ATX-S10Na (II) - and enhanced ICG-guided methods (Koyama et al., 2007b). These results suggest that the ATX-S10Na(II)-guided method is comparable to or possibly superior to the enhanced ICG-guided method. In addition, the number of ICG-stained nodes varies widely, since the number and distribution of stained nodes become larger and wider as the injection dose is increased (Ichikura et al., 2002). In the dual-mapping technique with dye and radioactive tracers, significant differences in distributions are noted between the two tracers (Hayashi et al., 2003; Karube et al., 2004). These findings raise the question of whether dye or radioactive traces flow into the lymphatic system in the same manner as metastatic cancer cells. ATX-S10Na (II) may resolve the issue, because it has a high specificity and affinity for tumor cells (Nakajima et al, 1992, 1998; Mori et al., 2000b). In the future, novel fluorescence-based reagents (Kim, S. et al., 2004; Ueno et al., 2005), including photosensi- tizers, will be developed as tracers that improve diagnostic accuracy in sentinel node navigation surgery.

7. Conclusion

A novel system using a hydrophilic photosensitizer ATX-S10Na (II) in combination with a fluorescence spectrolaparoscope is useful for the detection of cancer-containing sentinel nodes in an orthotopic xenograft animal model of human gastric carcinoma. ATX-S10Na(II) would serve as a novel tracer in sentinel node navigation surgery. This system has great potential application for the decision of minimally invasive surgery without radical extensive regional lymphadenectomy in early gastric carcinoma. A comparative study of ATX-S10Na (II) versus other dye tracers will determine whether the red-fluorescent tracer system is useful for lymphatic mapping in sentinel node navigation surgery for patients with early gastric carcinoma.
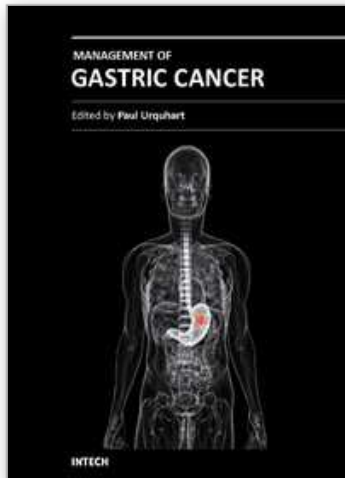
8. References

Bilchik, A.J.; Saha, S.; Wiese, D; Stonecypher, J.A.; Wood, T.F.; Sostrin, S.; Turner, R.R.; Wang, H.J.; Morton, D.L.; Hoon, D.S. (2001). Molecular staging of early colon cancer on the basis of sentinel node analysis: A multicenter phase II trial. *Journal of Clinical Oncology*, Vol.19, No.4, (February 2001), pp.1128–1136, ISSN 0732-183X

Fisher, A.M.; Murphree, A.L. & Gomer, C.J. (1995). Clinical and preclinical photodynam- ic therapy. *Lasers in Surgery and Medicine*, Vol.17, No.1, pp.2–31, ISSN 0196-8092

Flower, R.W. & Hochheimer. B.F. (1976). Indocyanine green dye fluorescence and infrared absorption choroidal angiography performed simultaneously with fluorescein angiography. *Johns Hopkins Medical Journal*, Vol.138, No.2, (February 1976), pp.33–42, ISSN 0021-7263

Fujihara, T.; Sawada, T.; Hirakawa, K.-Chung, Y.S.; Yashiro, M.; Inoue, T.; Sowa, M. (1998). Establishment of lymph node metastatic model for human gastric cancer in nude mice and analysis of factors associated with metastasis. *Clinical & Experimental Metastasis*, Vol.16, No.4, (May 1998), pp.389–398, ISSN 0262-0898

Hayashi, H.; Ochiai, T.; Mori, M.; Karube, T.; Suzuki, T.; Gunji, Y.; Hori, S.; Akutsu, N.; Matsubara, H.; Shimada, H. (2003). Sentinel lymph node mapping for gastric cancer using a dual procedure with dye- and gamma probe-guided techniques. *Journal of the American College of Surgeons*, Vol.196, No.1, (January 2003), pp.68–74, ISSN 1072-7515

Hiratsuka, M.; Miyashiro, I.; Ishikawa, O.; Furukawa, H.; Motomura, K.; Ohigashi, H.; Kameyama, M.; Sasaki, Y.; Kabuto, T.; Ishiguro, S.; Imaoka, S.; Koyama, H. (2001). Application of sentinel node biopsy to gastric cancer surgery. *Surgery*, Vol.129, No.3, (March 2001), pp.335-340, ISSN 0039- 6060

Hundley, J.C.; Shen, P.; Shiver, S.A.; Geisinger, K.R.; Levine, E.A. (2002). Lymphatic mapping for gastric adenocarci- noma. *American Surgeon*, Vol.68, No.11, (November 2002), pp.931–935, ISSN 0003-1348

Ichikura, T.; Morita, D.; Uchida, T.; Okura, E.; Majima, T.; Ogawa, T.; Mochizuki, H. (2002). Sentinel node concept in gastric carcinoma. *World Journal of Surgery*, Vol.26, No.3, (March 2002), pp.318–322, ISSN 0364-2313

Isozaki, H.; Kimura, T.; Tanaka, N.; Satoh, K.; Matsumoto, S.; Ninomiya, M.; Ohsaki, T.; Mori, M. (2004). An assessment of the feasibility of sentinel lymph node-guided surgery for gastric cancer. *Gastric Cancer*, Vol.7, No.3, pp.149–153

Karube, T.; Ochiai, T.; Shimada, H.; Nikaidou, T.; Hayashi, H. (2004). Detection of sentinel lymph nodes in gastric cancers based on immunohistochemical analysis of micrometastases. *Journal of Surgical Oncology*, Vol.87, No.1, (July 2004), pp.32–38, ISSN 0022-4790

Kim, S.; Lim, Y.T.; Soltesz, E.G.; De Grand, A.M.; Lee, J.; Nakayama, A.; Parker, J.A.; Mihaljevic, T.; Laurence, R.G.; Dor, D.M.; Cohn, L.H.; Bawendi, M.G.; Frangioni, J.V. (2004). Near-infrared fluorescent type II quantum dots for sentinel lymph node maping. *Nature Biotechnology*, Vol.22, No.1, (January 2004), pp.93–97, ISSN 1087-0156

Kim, M.C.; Kim, H.H.; Jung, G.J.; Lee, J.H.; Choi, S.R.; Kang, D.Y.; Roh, M.S.; Jeong, J.S. (2004). Lymphatic mapping and sentinel node biopsy using 99mTc tin colloid in gastric cancer. *Annals of Surgery*, Vol.239, No.3, (March 2004), pp.383–387, ISSN 0003-4932

Kitagawa, Y. & Kitajima, M. (2002). Gastrointestinal cancer and sentinel node navigation surgery. *Journal of Surgical Oncology*, Vol.79, No.3, (March 2002), pp.188–193, ISSN 0022-4790

Kohso, H.; Tatsumi, Y.; Fujino, H.; Tokita, K.; Kodama, T.; Kashima, K.; Kawai, K. (1990). An investigation of an infrared ray electronic endoscope with a laser diode light source. *Endoscopy*, Vol.22, No.5, (September 1990), pp.217–220, ISSN 0013-726X

Koyama, T.; Tsubota, A.; Nariai, K.; Yoshikawa, T.; Mitsunaga, M.; Sumi, M.; Nimura, H.; Yanaga, K.; Yumoto, Y.; Mabashi, Y.; Takahashi, H. (2007a). Detection of sentinel nodes by a novel red-fluorescent dye, ATX-S10Na(II), in an orthotopic xenograft rat model of human gastric carcinoma. *Lasers in Surgery and Medicine*, Vol39. No.1, (January 2007), pp.76–82, ISSN 0196-8092

Koyama, T.; Tsubota, A.; Nariai, K.; Mitsunaga, M.; Yanaga, K.; Takahashi, H. (2007b). Novel biomedical imaging approach for detection of sentinel nodes in an experimental model of gastric cancer. *British Journal of Surgery*, Vol.94, No.8, (August 2007), pp.996-1001, ISSN 0007-1323

Krag, D.; Weaver, D.; Ashikaga, T.; Moffat, F.; Klimberg, V.S.; Shriver, C.; Feldman, S.; Kusminsky, R.; Gadd, M.; Kuhn, J.; Harlow, S.; Beitsch, P. (1998). The sentinel node in breast cancer—a multicenter validation study. *New England Journal of Medicine*, Vol.339, No.14, (October 1998), pp.941–946, ISSN 0028-4793

Kvam, E., Stokke, T. & Moan, J. (1990). The lengths of DNA fragments light-induced in the presence of a photosensitizer localized at the nuclear membrane of human cells. *Biochimica et Biophysica Acta*, Vol.1049, No.1, (May 1990), pp.33–37, ISSN 0006-3002

Lee, J.H.; Ryu, K.W.; Kim, C.G.; Kim, S.K.; Choi, I.J.; Kim, Y.W.; Chang, H.J.; Bae, J.M.; Hong, E.K. (2005). Comparative study of the subserosal *versus* submucosal dye injection method for sentinel node biopsy in gastric cancer. *European Journal of Surgical Oncology*, Vol.31, No.9, (November 2005), pp.965–968, ISSN 0748-7983

Maruyama, K.; Sasako, M.; Kinoshita, T.; Sano, T.; Katai, H. (1999). Can sentinel node biopsy indicate rational extent of lymphadenectomy in gastric cancer surgery? Fundamental and new information on lymph-node dissection. *Langenbeck's Archives of Surgery*, Vol. 384, No.2, (April 1999), pp.149–157, ISSN 1435-2443

Masumoto, K.; Yamada, I.; Tanaka, H.; Fujise, Y.; Hashimoto, K. (2003). Tissue distribution of a new photosensitizer ATX-S10Na (II) and effect of a diode laser (670 nm) in photody- namic therapy. *Lasers in Medical Science*, Vol.18, No.3, pp.134–138, ISSN 0268-8921

Miwa, K.; Kinami, S.; Taniguchi, K.; Fushida, S.; Fujimura, T.; Nonomura, A. (2003). Mapping sentinel nodes in patients with early stage gastric carcinoma. *British Journal of Surgery*, Vol.90, No.2, (February 2003), pp.178–182, ISSN 0007-1323

Mori, M.; Sakata, I.; Hirano, T.; Obana, A.; Nakajima, S.; Hikida, M.; Kumagai, T. (2000a). Photodynamic therapy for experimental tumors using ATX-S10 (Na), a hydrophilic chlorin photosensitizer, and diode laser. *Japanese Journal of Cancer Research*, Vol.91, No.7, (July 2000), pp.753–759, ISSN 0910-5050

Mori, M.; Kuroda, T.; Obana, A.; Sakata, I.; Hirano, T.; Nakajima, S.; Hikida, M.; Kumagai, T. (2000b). In vitro plasma protein binding and cellu- lar uptake of ATX-S10 (Na), a hydrophilic chlorine photosensitizer. *Japanese Journal of Cancer Research*, Vol.91, No.8, (August 2000), pp.845–852, ISSN 0910-5050

Morton, D.L.; Wen, D.R.; Wong, J.H.; Economou, J.S.; Cagle, L.A.; Storm, F.K.; Foshag, L.J.; Cochran, A.J. (1992). Technical details of intraoperative lymphatic mapping for early stage melanoma. *Archives of Surgery*, Vol.127, No.4, (November 1991), pp.392–399, ISSN 0004-0010

Nakajima, S.; Sakata, I.; Takemura, T.; Maeda, T.; Hayashi, H.; Kubo, Y.; Samejima, N.; Koshimizu, K. (1992). Tumor localizing and photosensitiza- tion of photo-chlorin ATX-S10, In: *Photodynamic therapy and biomedical lasers*, Spinelli, P.; Fante, D.M.; Marchesini, R. (Ed.), 531–534, Elsevier Science, Amsterdam

Nakajima, S.; Sakata, I.; Hirano, T.; Takemura, T. (1998). Therapeutic effect of interstitial photody- namic therapy using ATX-S10 (Na) and a diode laser on radio-resistant SCCVII tumors of C3H/He mice. *Anti-cancer Drugs*, Vol.9, No.6, (July 1998), pp.539–543, ISSN 0959-4973

Natsugoe, S.; Mueller, J.; Stein, H.J.; Feith, M.; Hofler, H.; Siewert, J.R. (1998). Micrometastasis and tumor cell microin- volvement of lymph nodes from esophageal squamous cell carcinoma: Frequency, associated tumor characteristics, and impact on prognosis. *Cancer*, Vol. 83, No.5, (September 1998), pp.858–866, ISSN 0008-543X

Nimura, H.; Narimiya, N.; Mitsumori, N.; Yamazaki, Y.; Yanaga, K.; Urashima, M. (2004). Infrared ray electronic endoscopy combined with indocyanine green injection for detection of sentinel nodes of patients with gastric cancer. *British Journal of Surgery*, Vol.91, No.5, (May 2004), pp.575–579, ISSN 0007-1323

Noura, S., Yamamoto, H., Ohnishi, T.; Masuda, N.; Matsumoto, T.; Takayama, O.; Fukunaga, H.; Miyake, Y.; Ikenaga, M.; Ikeda, M.; Sekimoto, M.; Matsuura, N.; Monden, M. (2002). Comparative detection of lymph node micrometastases of stage II colorectal cancer by reverse transcriptase polymerase chain reaction and immunohistochem- istry. *Journal of Clinical Oncology*, Vol.20, No. 20, (October 2002), pp.4232–4241, ISSN 0732-183X

Osaka, H.; Yashiro, M.; Sawada, T.; Katsuragi, K.; Hirakawa, K. (2004). Is a lymph node detected by the dye-guided method a true sentinel node in gastric cancer? *Clinical Cancer Research*, Vol.10, No.20, (October 2004), pp.6912–6918, ISSN 1078-0432

Ryu, K.W.; Lee, J.H.; Kim, H.S.; Kim, Y.W.; Choi, I.J.; Bae, J.M.. (2003). Prediction of lymph nodes metastasis by sentinel node biopsy in gastric cancer. *European Journal of Surgical Oncology*, Vol.29, No.10, (December 2003), pp.895–899, ISSN 0748-7983

Sharman, W.M.; Allen, C.M. & van Lier, J.E. (1999). Photodynamic therapeutics: basic principles and clinical applications. *Drug Discovery Today*, Vol.4, No.11, (November 1999), pp.507–517, ISSN 1359-6446

Simsa, J.; Hoch, J.; Leffler, J.; Schwarz, J.; Pospisil, R.; Vajtrova, R. (2003). Sentinel node biopsy in gastric cancer: preliminary results. *Acta Chirurgica Belgica*, Vol.103, No.3, (June 2003), pp.270–273, ISSN 0001-5458

Sobin, L.H. (2003). TNM, sixth edition: New developments in general concepts and rules. *Seminars in Surgical Oncology*, Vol.21, No.1, (August 2003), pp.19–22, ISSN 1098-2388

Song, X; Wang, L.; Chen, W.; Pan, T.; Zhu, H.; Xu, J.; Jin, M.; Finley, R.K.; Wu, J. (2004). Lymphatic mapping and sentinel node biopsy in gastric cancer. *American Journal of Surgery* Vol.187, No.2, (February 2004), pp.270–273, ISSN 0002-9610

Tanaka, K., Tonouchi, H., Kobayashi, M.; Konishi, N.; Ohmori, Y.; Mohri, Y.; Kusunoki, M. (2004). Laparoscopically assisted total gastrectomy with sentinel node biopsy for early gastric cancer: Preliminary results. *American Surgeon*, Vol.70, No.11, (November 2004), pp.976–981, ISSN 0003-1348

Ueno, H.; Hihara, J.; Shimizu, K.; Osaki, A.; Yamashita, Y.; Yoshida, K.; Toge, T. (2005). Experimental study on fluorescent microspheres as a tracer for sentinel node detection. *Anticancer Research*, Vol.25, No.2A, (March-April 2005), pp.821–825, ISSN 0250-7005

van der Veen, H.; Hoekstra, O.S.; Paul, M.A.; Cuesta, M.A.; Meijer, S. (1994). Gamma probe-guided sentinel node biopsy to select patients with melanoma for lymphadenectomy. *British Journal of Surgery*, Vol.81, No.12, (December 1994), pp.1769–1770, ISSN 0007-1323

Veronesi, U.; Paganelli, G.; Galimberti, V.; Viale, G.; Zurrida, S.; Bedoni, M.; Costa, A.; de Cicco, C.; Geraghty, J.G.; Luini, A.; Sacchini, V.; Veronesi, P. (1997). Sentinel-node biopsy to avoid axillary dissection in breast cancer with clinically negative lymph-nodes. *Lancet*, Vol.349, No.9069, (June 1997), pp.1864–1867, ISSN 0140-6736

Management of Gastric Cancer

Edited by Dr Nabil Ismaili

Gastric cancer is the fifth most common cancer and the second most common cause of cancer death worldwide. More than 50% of the patients have advanced disease at diagnosis and in this case the disease has a poor outcome. The staging of gastric cancers is based on endoscopic ultrasound, computed tomography, magnetic resonance imaging, positron emission tomography, in addition to the laparoscopic staging. Many improvements in the surgical techniques have been seen in the last decade. Laparoscopic surgery is an emerging approach which offers important advantages: less blood loss, reduced postoperative pain, accelerated recovery, early return to normal bowel function and reduced hospital stay. D1 lymphadenectomy, with a goal of examining 15 or greater lymph nodes is a standard. D2 dissection is considered as a standard in several institutions especially in eastern Asia. Perioperative chemotherapy and adjuvant concurrent radiochemotherapy are recognized as standards treatments. Palliative chemotherapy is the mainstay treatment of advanced stages of the disease (metastatic and non-operable tumors). Despite these treatment advances, the prognosis of gastric cancer remains poor with a 5-year survival ranging from 10 to 15% in all stages combined.

How to reference

In order to correctly reference this scholarly work, feel free to copy and paste the following:

Akihito Tsubota (2011). Novel Biomedical Imaging Approach for Detection of Sentinel Nodes in an Orthotopic Xenograft Rat Model of Human Gastric Carcinoma, Management of Gastric Cancer, Dr Nabil Ismaili (Ed.), ISBN: 978-953-307-344-6, InTech, Available from: http://www.intechopen.com/books/management-of-gastric-cancer/novel-biomedical-imaging-approach-for-detection-of-sentinel-nodes-in-an-orthotopic-xenograft-rat-mod

INTECH
open science | open minds